

NANO IDEA

Open Access



# Synthesis of Water-Soluble Antimony Sulfide Quantum Dots and Their Photoelectric Properties

Jiang Zhu<sup>1</sup>, Xuelian Yan<sup>1</sup> and Jiang Cheng<sup>1,2\*</sup>

## Abstract

Antimony sulfide ( $\text{Sb}_2\text{S}_3$ ) has been applied in photoelectric devices for a long time. However, there was lack of information about  $\text{Sb}_2\text{S}_3$  quantum dots (QDs) because of the synthesis difficulties. To fill this vacancy, water-soluble  $\text{Sb}_2\text{S}_3$  QDs were prepared by hot injection using hexadecyltrimethylammonium bromide (CTAB) and sodium dodecyl sulfate (SDS) mixture as anionic-cationic surfactant, alkanol amide (DEA) as stabilizer, and ethylenediaminetetraacetic acid (EDTA) as dispersant. Photoelectric properties including absorbing and emission were characterized by UV-Vis-IR spectrophotometer and photoluminescence (PL) spectroscopic technique. An intensive PL emission at 880 nm was found, indicating  $\text{Sb}_2\text{S}_3$  QDs have good prospects in near-infrared LED and near-infrared laser application.  $\text{Sb}_2\text{S}_3$  QD thin films were prepared by self-assembly growth and then annealed in argon or selenium vapor. Their band gaps ( $E_g$ s) were calculated according to transmittance spectra. The  $E_g$  of  $\text{Sb}_2\text{S}_3$  QD thin film has been found to be tunable from 1.82 to 1.09 eV via annealing or selenylation, demonstrating the good prospects in photovoltaic application.

**Keywords:**  $\text{Sb}_2\text{S}_3$ , Water-soluble quantum dot, Near-infrared emission, Photovoltaic material

## Background

Quantum dots (QDs) have received a great deal of attention over the past decade owing to their manipulated photoelectric properties and superior solution processibility for device engineering [1–3]. Typically, lead compound QDs such as PbS and lead halide perovskites have recently emerged as promising candidate materials in photoelectric applications such as photovoltaics, OLEDs, lasing, and photodetectors due to their simple synthesis and satisfactory performance [4–6]. Besides, a range of semiconductor QDs, such as CdS, CdSe, ZnS, ZnSe, HgTe, CuInSe<sub>2</sub>, CuInS<sub>2</sub>, and CdHgTe, and base device have been reported everywhere.

$\text{Sb}_2\text{S}_3$  has been known as the commonest antimony sulfide, which is a promising semiconductor material for

photoelectric semiconductor manufacturing [7, 8]. It has a moderate band gap approximately 1.7–1.8 eV in crystalline form (stibnite). Curiously, the band gap is tunable at the range of 1.1–1.8 eV when sulfur is partly replaced by selenium [9]. Naturally,  $\text{Sb}_2\text{S}_3$  is a multifunction material that could be used as an absorber or a sensitizer for photovoltaic device, photochemical catalysis, and photo-detector. Besides, Sb and S are comparatively abundant, low-cost, and low-toxicity elements, making it potential for large-scale application. Antimony sulfide has a unique processibility. They can be vacuum-evaporated at a low temperature (~400 °C) or solution-processed using various materials.  $\text{Sb}_2\text{S}_3$  was usually applied in sensitized solar cells. Using a thioacetamide-treated  $\text{Sb}_2\text{S}_3$  sensitizer deposited by chemical solution deposition (CBD), a sensitized hybrid solar cell with a power conversion efficiency (PCE) of 7.5% was realized [10]. Recently, solution-processed planar heterojunction solar cells with a simple structure achieved a very satisfying PCE of 4.3%, in which an  $\text{Sb}_2\text{S}_3$  film was prepared by conventional spin-cast technique with a precursor containing  $\text{Sb}_2\text{O}_3$ ,  $\text{CS}_2$ , and n-butylamine [7]. Nanostructure  $\text{Sb}_2\text{S}_3$  synthesized by

\* Correspondence: cheng20120027@hotmail.com

<sup>1</sup>Co-Innovation Center for Micro/Nano Optoelectronic Materials and Devices, College of Materials and Chemical Engineering, Chongqing University of Arts and Sciences, No. 319, Honghe Road, Yongchuan District, Chongqing 402160, People's Republic of China

<sup>2</sup>State Key Laboratory of Advanced Chemical Power Sources, No. 705, Zhonghuabei Road, Honghuagang District, Zunyi 563003, Guizhou Province, People's Republic of China

solution method was widely applied for high-performance photodetectors [11–13].  $\text{Sb}_2\text{S}_3$  NW-based photodetectors exhibited a good photo-response in a wide spectral range from 300 to 800 nm. Especially at 638 nm, they showed optimal values with a high current ON/OFF ratio about 210, a spectral responsivity of 1152 A/W, a detectivity of  $2 \times 10^{13}$  Jones, and the rise and fall times of about 37 ms [11]. Solution-processed  $\text{Sb}_2\text{S}_3$  nanorod was usually used as an efficient photocatalyst for dye degradation [14] and high-performance sodium-ion batteries [15]. Unfortunately, there was few reported information about  $\text{Sb}_2\text{S}_3$  QDs.

We believe  $\text{Sb}_2\text{S}_3$  zero-dimensional materials must have unusual optical and electrical properties comparing to multidimensional materials because of the quantum confinement effect. To fill this vacancy, the present paper firstly reported the synthesis of water-soluble antimony sulfide QDs using CTAB and SDS mixture as anionic-cationic surfactant, DEA as stabilizer, and EDTA as dispersant under 120 °C oil bath conditions. In order to overcome the interference of hydroxyl, the reaction was conducted in anhydrous 2-methoxyethanol instead of water. These precursors are nontoxic, odorless, and inexpensive compared with conventional additives [16, 17]. Before the substantial application, the structural, optical, and electrical properties were studied herein.

### Experimental

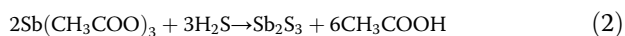
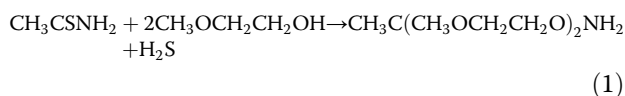
$\text{Sb}_2\text{S}_3$  QDs were synthesized by rapid hot injection method. In a typical procedure for the preparation, SDS (0.05 mmol, 99.5%), CTAB (0.05 mmol, 99.5%), EDTA (0.2 mmol, 99.5%), and DEA (4 ml, 99.9%) were mixed in the 100-ml anhydrous 2-methoxyethanol and dissolved after 20 min magnetic stirring in 120 °C oil bath. Next, 0.5 mmol thioacetamide (TAA) was dissolved in the hot solution. Then, 2 ml antimony acetate—acetic acid solution (0.25 M)—was injected to the precursor solution with magnetic stirring. Immediately, the solution turned from transparent to bright yellow, indicating the formation of sulfide. The container was then turned into ice bath to terminate reaction. The final product was centrifuged at 15000 rpm for 10 min and then washed with isopropanol repeatedly for at least three times and finally was centrifuged at 6000 rpm for 5 min to remove the coarse particles.

$\text{Sb}_2\text{S}_3$  QDs were vacuum-dried at room temperature and then tested using a simultaneous thermal analyzer (STA 449 F3, NETZSCH). Crystal structure was characterized by X-ray diffraction (XRD, Bruker D8). Composition measurement was carried out by an energy-dispersive spectrometer (EDS, EDAX Inc.).  $\text{Sb}_2\text{S}_3$  powder (99.99%, Aladdin) was used as standard for the calibration of EDS measurements. Nanoscale information of QDs was characterized by high-resolution transmission electron microscopy

(HRTEM; Zeiss Libra200) with selected-area electron diffraction (SAED). The emission spectra were recorded by using photoluminescence spectroscopic technique (PL, Horiba iHR550) with an He–Ne laser (325 nm) as excitation source. Optical transmittance spectra were carried out on QD dispersion and films by using a UV-Vis-IR spectrophotometer (Agilent Cary 5000).

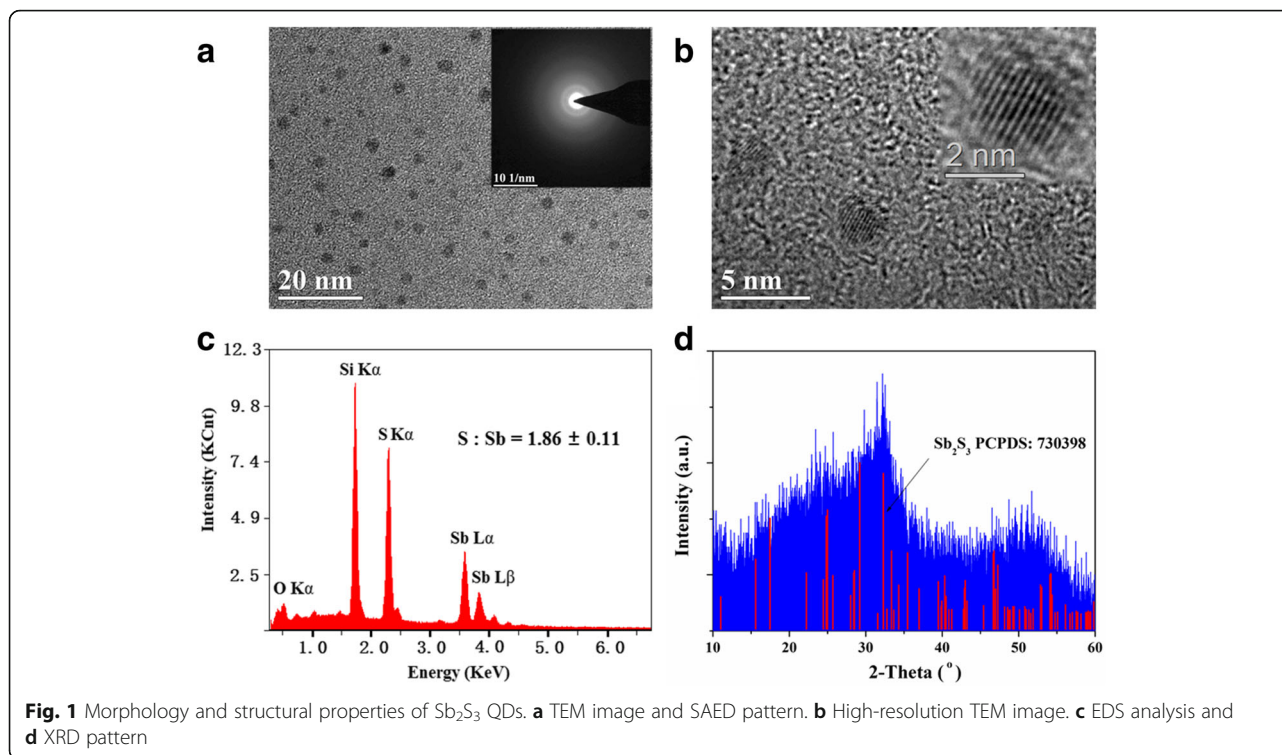
### Results and Discussion

The synthesis of  $\text{Sb}_2\text{S}_3$  QDs is a low-cost, easy operation and repeatable process. The chemical reaction can be described in the following two simple reaction equations.



According to the LaMer model [18], separation of nucleation and crystal growth stages is the main requirement for small particle formation with narrow size distributions. At the early stage of this reaction, the solution containing equimolar SDS/CTAB tended to form relatively larger catanionic vesicles rather than mixed micelles [16]. The reaction between  $\text{S}^{2-}$  and  $\text{Sb}^{2+}$  took place rapidly, leading to the explosive nucleation. Next, due to the chelation effect, the formation of the metal ions-ETDA complexes reduces the free metal ion concentration [19]. Thus, the grain growth was effectively inhibited, remaining  $\text{Sb}_2\text{S}_3$  QDs in the solution.

Effect of temperature and reaction time on the morphologies of QDs has been studied first. We found the shape and size were nearly invariable when the temperature varied from 90 to 120 °C and the reaction time was controlled from 30 s to 15 min. Figure 1a, b shows a TEM image and a high-resolution image of the sample synthesis at 120 °C. The images reveal good monodispersity of QDs with a uniform spherical shape, and the diameters mainly lie in the range of 3 to 5 nm. The high-resolution image shows a clear lattice fringe, revealing each particle is a monocrystalline quantum. SAED exhibits some concentric circles with indistinct boundaries, indicating the synthesized nanomaterial has a low crystallinity. Chemical compositions were analyzed by EDS as shown in Fig. 1c. A quantitative elemental EDS analysis of QDs reveals the average atom ratio (S%:Sb%) is 1.68, indicating the stoichiometric ratio of sulfur element is slightly higher. We deduced that some sulfur was chemisorbed or physically adsorbed on the surface of QDs. Figure 1d shows XRD spectrum of vacuum-dried QDs. Roughly, XRD pattern is matched to orthorhombic  $\text{Sb}_2\text{S}_3$  (JCPDS no. 73-0393), confirming

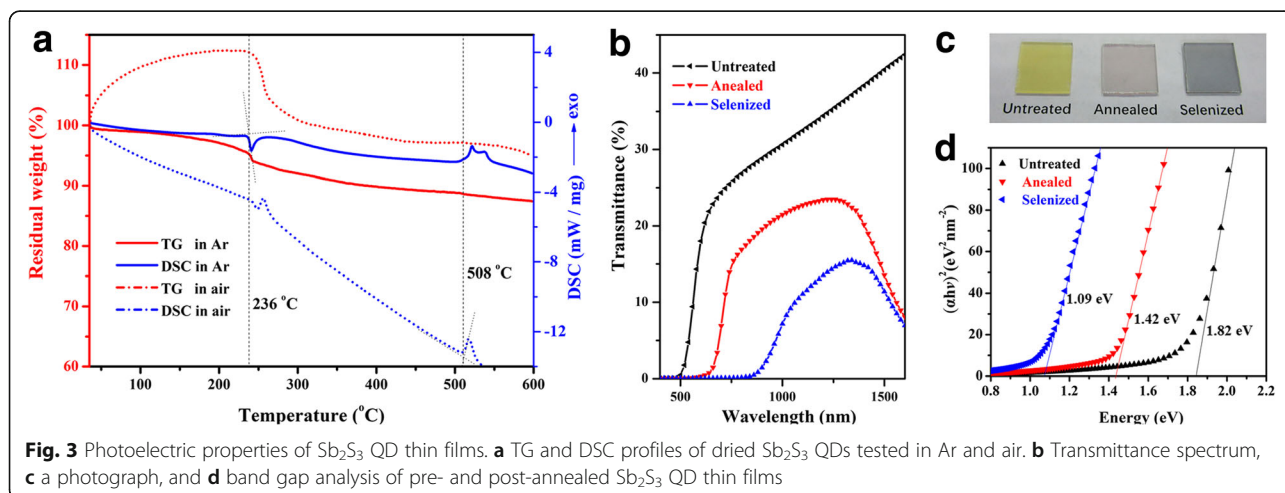
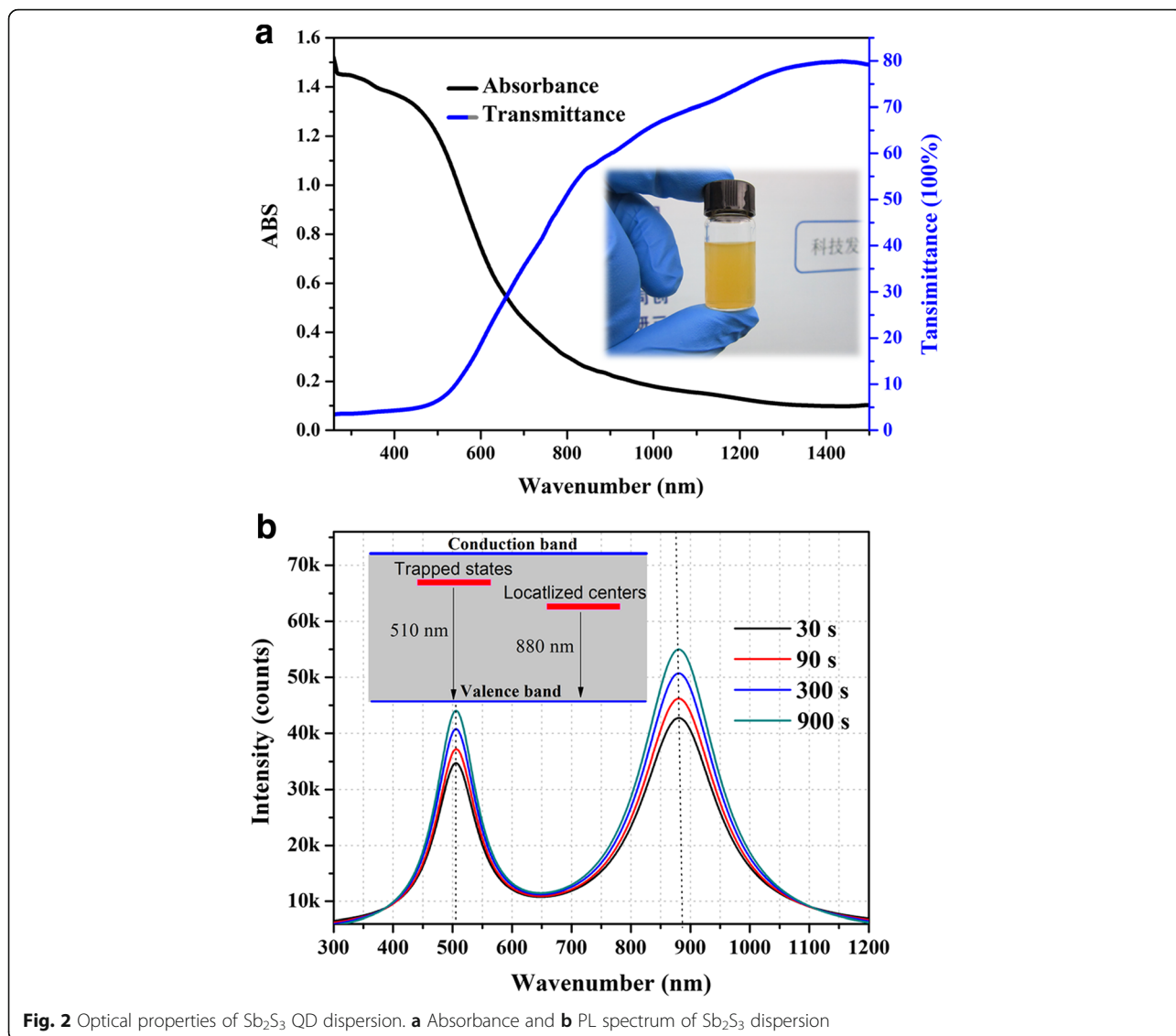


the results of EDS analysis. The indistinct XRD peaks indicate the low crystallinity which is quite agreeable with the SAED pattern.

Optical absorption of QDs-isopropanol dispersion was measured by Agilent Cary 5000 spectrophotometer. As we see in Fig. 2a,  $\text{Sb}_2\text{S}_3$  QDs dispersion is bright yellow and has a broad absorption at nearly the whole visible range. It shows a nearly complete absorption at short wavelength from 300 to 500 nm and a high transmittance at a near-infrared region. Figure 2b shows the photoluminescence (PL) spectra of dispersion with a concentration of 2 mg/ml where  $\text{Sb}_2\text{S}_3$  was prepared with different reaction times. PL spectra for all  $\text{Sb}_2\text{S}_3$  samples exhibit two distinct emission peaks at around 510 nm (2.43 eV) and 880 nm (1.41 eV), which is significantly different from nanostructured  $\text{Sb}_2\text{S}_3$  prepared by chemical solution deposition (CBD) [20]. According to the previous report, CBD-synthesized  $\text{Sb}_2\text{S}_3$  nanocrystals show a weak band edge emission peaked at around 610 nm (2.03 eV) presumably resulting from excitons and a sulfur vacancy-related strong emission peaked at 717 nm (1.72 eV). For water-soluble  $\text{Sb}_2\text{S}_3$  QDs here, the green emission around 510 nm presumably results from excitons [21, 22], which is well known and widely reported for semiconductor nanocrystals [23], suggesting the quantum size effect (QSE) brings a broader band gap for  $\text{Sb}_2\text{S}_3$  QDs. The near-infrared emission around 880 nm may be attributed to the presence of stoichiometry-related point defects. According to the

EDS analysis discussed above, the average atom ratio ( $\text{S}:\text{Sb}\%$ ) is 1.68; we deduced sulfur is excessive and the type of point defects here is likely to be antimony vacancies ( $V_{\text{Sb}}^+$ ). Careful observation of curves reveals that the emission peaked at 880 nm of  $\text{Sb}_2\text{S}_3$  QDs prepared with long reaction time exhibits slightly blue shift compared with rapid synthesized QDs. This shift is probable from the slight improvement of stoichiometric ratio. The intensive PL emission and high transmittance at a near-infrared region point that  $\text{Sb}_2\text{S}_3$  QDs have good prospects in the fabrication of near-infrared LEDs [17, 24] and near-infrared lasers applied in sensing and probing.

To further study the applications of  $\text{Sb}_2\text{S}_3$  QDs in semiconductor processing,  $\text{Sb}_2\text{S}_3$  films were prepared by self-assembly growth on glass from a 5 mg/ml QDs-isopropanol dispersion. Before anneal treatment, thermogravimetric analysis was employed for the stability test. According to TG and DSC profiles for the vacuum-dried QDs shown in Fig. 3a,  $\text{Sb}_2\text{S}_3$  QDs have an approximately 12% weight increment beginning from room temperature, indicating these have a high activity and probably been partly oxidized or surface-adhered.  $\text{Sb}_2\text{S}_3$  QDs exhibit a relative stability in argon at room temperature and then show the first obvious weight loss followed by the excess S removal started at 236 °C. The melting point of  $\text{Sb}_2\text{S}_3$  QDs was measured to be 508 °C, which is remarkably lower than that of crystalline  $\text{Sb}_2\text{S}_3$  powder (550 °C, Sigma Aldrich). We noticed there was a gradual slow weight loss at the whole test temperature range accompanied by S



constituent loss.  $\text{Sb}_2\text{S}_3$  QD films anneal treatment in Ar and Se vapor was subsequently studied. Optical transmission spectra for untreated, annealed, and selenized films are shown in Fig. 3b, and the photograph of the three samples is shown in Fig. 3c. For the annealed and selenized samples, both of them were treated at 250 °C for 5 min. The absorbing edges of the annealed and selenized samples were shifted from 500 nm to 650 and 850 nm, respectively. Because both  $\text{Sb}_2\text{S}_3$  and  $\text{Sb}_2\text{Se}_3$  are direct band gap semiconductor [24, 25], the average band gap could be calculated by the formula:

$$\alpha = (A/h\nu) \times (h\nu - E_g)^{1/2} \quad (3)$$

where  $A$  is a constant,  $h$  is Planck's constant, and  $\nu$  is the frequency of the incident photon. We fitted the linear zone by plotting  $(\alpha h\nu)^2$  versus  $(h\nu)$  and calculated the average  $E_g$  as shown in Fig. 3. As we see, the  $E_g$  of untreated sample was 1.82 eV and decreased to 1.42 eV after 5 min annealing at 250 °C. The variation of  $E_g$  indicates the crystallinity of  $\text{Sb}_2\text{S}_3$  has been improved with an order-disorder transformation accompanied by the removal of excessive S element [26]. For the selenized sample, the  $E_g$  decreased to a minimum of 1.09 eV, which is very close to crystalline silicon. Quantitative elemental EDS analysis revealed that  $\text{Sb}_2\text{S}_3$  was transformed to  $\text{Sb}_2(\text{S}_{1-x}\text{Se}_x)_3$  and finally to  $\text{Sb}_2\text{Se}_3$  after the most of sulfur have been replaced by selenium [7, 9]. Because the selenylation is lower than 250 °C, we believe it was beneficial for the manufacturing and performance improving of flexible devices. As we know, the optimum band gap for solar cell absorber was 1.45 eV. Thus, the annealed and selenized  $\text{Sb}_2\text{S}_3$  QD films are good candidates for photovoltaic absorber materials.

## Conclusions

A novel way to synthesize water-soluble  $\text{Sb}_2\text{S}_3$  QDs was developed by hot injection using CTAB and SDS mixture as anionic-cationic surfactant, DEA as stabilizer, and EDTA as dispersant. The synthesis process is easy to operate and repeatable. All the reagents and additives are nontoxic, odorless, and inexpensive.  $\text{Sb}_2\text{S}_3$  QDs have an intensive PL emission at 880 nm and a high transmittance at a near-infrared region, indicating it has good prospects in the fabrication of near-infrared LEDs and near-infrared lasers.  $\text{Sb}_2\text{S}_3$  QDs show a good monodispersity and processibility, which can be deposited to form  $\text{Sb}_2\text{S}_3$  films. The  $E_g$  of  $\text{Sb}_2\text{S}_3$  QD films could be turned to 1.42 and 1.09 eV after annealing treatment in Ar or Se vapor at lower than 250 °C, demonstrating their good prospects in photovoltaic application.

## Abbreviations

CBD: Chemical solution deposition; CTAB: Hexadecyltrimethylammonium bromide; DEA: Alkanol amide; DSC: Differential scanning calorimeter; EDS: Energy-dispersive spectrometer; EDTA: Ethylenediaminetetraacetic acid; HRTEM: High-resolution transmission electron microscopy; LED: Light-emitting diode; OLED: Organic light-emitting diode; PL: Photoluminescence; QD: Quantum dot; QSE: Quantum size effect; SAED: Selected-area electron diffraction; SDS: Sodium dodecyl sulfate; STA: Simultaneous thermal analyzer; TAA: Thioacetamide; TGA: Thermogravimetric analysis; XRD: X-ray diffraction

## Acknowledgements

The authors thank Co-Innovation Center for Micro/Nano Optoelectronic Materials and Devices for the financial support. Wuhan National Laboratory for Optoelectronics and Guangzhou Chemical Union Quality Testing Technology Co., Ltd. are also acknowledged for the characterization support.

## Funding

This work was supported by National Natural Science Foundation of China (grant no. 61505018, 21603020, and 51503022), Natural Science Foundation of Yongchuan District (grant no. Ycstc, 2016nc1001), Technology Project from Chongqing Education Committee (grant no. KJ1401113 and KJ1501116), and Chongqing Science and Technology Commission (grant no. cstc2016jcyjys0006 and cstc2016jcyjA0451).

## Declarations

This study has nothing to do with human participants or health-related outcomes.

## Authors' Contributions

ZJ designed and conducted the experiments and analyses and drafted the manuscript. XY prepared the CZTS NPs and performed the characterization of  $\text{Sb}_2\text{S}_3$  QDs. JC modified the manuscript and supervised all the projects. All authors read and approved the final manuscript.

## Competing Interests

The authors declare that they have no competing interests.

## Publisher's Note

Springer Nature remains neutral with regard to jurisdictional claims in published maps and institutional affiliations.

Received: 21 November 2017 Accepted: 21 December 2017

Published online: 15 January 2018

## References

- Shi G, Wang Y, Liu Z, Han L, Liu J, Wang Y, Lu K, Chen S, Ling X, Li Y (2017) Stable and highly efficient PbS quantum dot tandem solar cells employing a rationally designed recombination layer. *Adv Energy Mater* 7:1602667–1602667
- Tong X, Zhou Y, Jin L, Basu K, Adhikari R, Selopal GS, Tong X, Zhao H, Sun S, Vomiero A, Wang AM, Roseia F (2017) Heavy metal-free, near-infrared colloidal quantum dots for efficient photoelectrochemical hydrogen generation. *Nano Energy* 31:441–449
- Tong X, Kong XT, Zhou Y, Navarro-Pardo F, Selopal GS, Sun S, Govorov AO, Zhao H, Wang ZM, Rosei F (2017) Near-infrared, heavy metal-free colloidal "giant" core/shell quantum dot. *Adv Energy Mater*. <https://doi.org/10.1002/aenm.201701432>
- Mcdonald SA, Konstantatos G, Zhang S, Cyr PW, Klem EJ, Levina L, Sargent EH (2005) Solution-processed PbS quantum dot infrared photodetectors and photovoltaics. *Nat Mater* 4:138–138
- Song J, Li J, Li X, Xu L, Dong Y, Zeng H (2015) Nanocrystals: quantum dot light-emitting diodes based on inorganic perovskite cesium lead halides ( $\text{CsPbX}_3$ ). *Adv Mater* 27:7161–7167
- Im JH, Lee CR, Lee JW, Park SW, Park NG (2011) 6.5% efficient perovskite quantum-dot-sensitized solar cell. *Nano* 3:4088–4088
- Wang X, Li J, Liu W, Yang S, Zhu C, Chen T (2017) A fast chemical approach towards  $\text{Sb}_2\text{S}_3$  film with a large grain size for high-performance planar heterojunction solar cells. *Nanoscale* 9:3386–3390
- Gödel KC, Choi YC, Roose B, Sadhanala A, Snaith HJ, Seok SI, Steiner U, Pathak SK (2015) Efficient room temperature aqueous  $\text{Sb}_2\text{S}_3$  synthesis

- for inorganic-organic sensitized solar cells with 5.1% efficiencies. *Chem Commun* 51:8640–8643
9. Zhang Y, Li J, Jiang G, Liu W, Yang S, Zhu C, Chen T (2017) Selenium-graded  $\text{Sb}_2(\text{S}_{1-x}\text{Se}_x)_3$  for planar heterojunction solar cell delivering a certified power conversion efficiency of 5.71%. *Solar RRL*. <https://doi.org/10.1002/solr.201700017>
  10. Choi YC, Lee DU, Noh JH, Kim EK, Seok SI (2014) Highly improved  $\text{Sb}_2\text{S}_3$  sensitized-inorganic-organic heterojunction solar cells and quantification of traps by deep-level transient spectroscopy. *Adv Funct Mater* 24:3587–3592
  11. Zhong M, Wang X, Liu S, Li B, Huang L, Cui Y, Li J, Wei Z (2017) High-performance photodetectors based on  $\text{Sb}_2\text{S}_3$  nanowires: wavelength dependence and wide temperature range utilization. *Nano* 9:12364–12364
  12. Zhang K, Luo T, Chen H, Lou Z, Shen G (2017) Au-nanoparticles-decorated  $\text{Sb}_2\text{S}_3$  nanowire based flexible ultraviolet/visible photodetectors. *J Mater Chem* 5:3330–3335
  13. Chao J, Liang B, Hou X, Liu Z, Xie Z, Liu B, Song W, Chen G, Chen D, Shen G (2013) Selective synthesis of  $\text{Sb}_2\text{S}_3$  nanoneedles and nanoflowers for high performance rigid and flexible photodetectors. *Opt Express* 21:13639–13647
  14. Sun M, Li D, Li W, Chen Y, Chen Z, He Y, Fu X (2008) New photocatalyst,  $\text{Sb}_2\text{S}_3$ , for degradation of methyl orange under visible-light irradiation. *J Phys Chem C* 112:18076–18081
  15. Hou H, Jing M, Huang Z, Yang Y, Zhang Y, Chen J, Wu Z, Ji X (2015) One-dimensional rod-like  $\text{Sb}_2\text{S}_3$ -based anode for high-performance sodium-ion batteries. *ACS Appl Mater Inter* 7:19362–19369
  16. Jiao Y, Gao X, Lu J, Chen Y, Zhou J, Li X (2012) A novel method for  $\text{PbS}$  quantum dot synthesis. *Mater Lett* 72:116–118
  17. Deng D, Zhang W, Chen X, Liu F, Zhang J, Gu Y, Hong J (2009) Facile synthesis of high-quality, water-soluble, near-infrared-emitting  $\text{PbS}$  quantum dots. *Eur J Inorg Chem* 2009:3440–3446
  18. Sugimoto T (1987) Preparation of monodispersed colloidal particles. *Adv Colloid Interf* 150:208–225
  19. Chiu G, Meehan EJ (1974) The preparation of monodisperse lead sulfide sols. *J Colloid Interf Sci* 83:309–310
  20. Kulkarni AN, Prasad MBR, Ingle RV, Pathan HM, Eldesoky GE, Naushad M, Patil RS (2015) Structural and optical properties of nanocrystalline  $\text{Sb}_2\text{S}_3$  films deposited by chemical solution deposition. *Opt Mater* 46:536–541
  21. Ma X, Xu F, Benavides J, Cloutier SG (2012) High performance hybrid near-infrared LEDs using benzenedithiol cross-linked  $\text{PbS}$ . *Colloidal Nanocrystals* 13:525–531
  22. Lim J, Shin K, Kim HW, Lee C (2004) Effect of annealing on the photoluminescence characteristics of  $\text{ZnO}$  thin films grown on the sapphire substrate by atomic layer epitaxy. *Mater Sci Eng* 107:301–304
  23. Park WD (2010) Photoluminescence of nanocrystalline  $\text{CdS}$  thin films prepared by chemical bath deposition. *Trans Electr Electron Mater* 11:170–173
  24. Liu X, Chen J, Luo M, Leng M, Xia Z, Zhou Y, Qin S, Xue DJ, Lv L, Huang H (2014) Thermal evaporation and characterization of  $\text{Sb}_2\text{Se}_3$  thin film for substrate  $\text{Sb}_2\text{Se}_3/\text{CdS}$  solar cells. *ACS Appl Mater Inter* 6:10687–10695
  25. Yang B, Xue DJ, Leng M, Zhong J, Wang L, Song H, Zhou Y, Tang J (2014) Hydrazine solution processed  $\text{Sb}_2\text{S}_3$ ,  $\text{Sb}_2\text{Se}_3$  and  $\text{Sb}_2(\text{S}_{1-x}\text{Se}_x)_3$  film: molecular precursor identification, film fabrication and band gap tuning. *SCI REP-UK* 5:10978
  26. Ye ZY, Lu HL, Geng Y, Gu YZ, Xie ZY, Zhang Y, Sun QQ, Ding SJ, Zhang DW (2013) Structural, electrical, and optical properties of Ti-doped  $\text{ZnO}$  films fabricated by atomic layer deposition. *Nanoscale Res Lett* 8:108

Submit your manuscript to a SpringerOpen<sup>®</sup> journal and benefit from:

- Convenient online submission
- Rigorous peer review
- Open access: articles freely available online
- High visibility within the field
- Retaining the copyright to your article

---

Submit your next manuscript at ► [springeropen.com](http://springeropen.com)

---